PROCEEDINGS OF SCIENCE

# Recent Results in Higgs Physics

**Tatsuya Masubuchi**[a,*] **on behalf of the ATLAS and CMS Collaborations**

[a] *International center of elementary particle physics, The University of Tokyo, 7-3-1 Hongo Bunkyo-ku, Tokyo 113-0033, Japan*

*E-mail:* tatsuya.masubuchi@cern.ch

These proceedings report on recent results of the Higgs physics by ATLAS and CMS at the Large Hadron Collider. All Run 2 analysis results are based on the full Run 2 dataset, corresponding to an integrated luminosity of approximately 140 fb$^{-1}$ at $\sqrt{s}$ = 13 TeV. Various measurements of Higgs properties: mass, width, couplings, cross sections and self-coupling are performed. First Run 3 Higgs cross section measurement is obtained using 2022 data, corresponding to approximately 30 fb$^{-1}$ at the $\sqrt{s}$ = 13.6 TeV. No significant deviation from the Standard Model on the Higgs boson properties is observed.

ATL-PHYS-PROC-2023-080
06 November 2023

**** The European Physical Society Conference on High Energy Physics (EPS-HEP2023), ****
**** 21-25 August 2023 ****
**** University of Hamburg, Hamburg, Germany ****

*Speaker





PoS(EPS-HEP2023)006

## 1. Introduction

In 2012, ATLAS and CMS discovered a Higgs boson [1, 2] at the Large Hadron Collider (LHC) [3]. The discovery of the Higgs boson filled the last particle predicted by the Standard Model (SM). At the same time, this discovery opens many questions not solved in the SM. The Higgs sector is the most vulnerable in the SM. 15 parameters out of 19 in the SM are related to the Higgs sector. ATLAS [4] and CMS [5] have measured Higgs boson properties in Run 1, and Run 2. There are several extraordinary achievements during Run2: the observation of the Higgs boson production in association with a top quarks [6, 7], the observation of the Higgs boson decaying into a pair of bottom quarks [8, 9], the evidence of the interaction between Higgs boson and muon [10, 11], and the evidence of Higgs boson decaying into $\ell\ell\gamma$ [12].

These proceedings report the highlight of the recent Higgs boson property measurements using full Run 2 dataset corresponding to roughly 140 fb$^{-1}$ at $\sqrt{s}$= 13 TeV collected by the ATLAS and CMS experiments and using Run 3 dataset of 2022 at $\sqrt{s}$ = 13.6 TeV collected by the ATLAS experiment [13].

## 2. Higgs mass measurement

ATLAS measures Higgs boson mass using $H \to \gamma\gamma$ channel which has excellent mass resolution due to precise photon energy scale and resolution calibrations. However, they were still the dominant systematic uncertainties for the mass measurement in the previous analysis [14]. ATLAS improves the calibration method of the photon energy scale and resolution, in particular, in-situ calibration using $Z \to ee$ events providing a significant reduction of the systematic uncertainties [15]. The systematic uncertainty of photon calibration is reduced by a factor of four. The measured Higgs boson mass is 125.17±0.11(stat.)±0.09(syst.) GeV in Run 2 dataset and 125.22±0.11(stat.)±0.09(syst.) GeV combined with Run 1 dataset [14]. ATLAS combined mass measurement of $H \to \gamma\gamma$ with that of the $H \to ZZ^* \to 4\ell$ which provides another best mass measurement because of the excellent lepton energy and momentum calibration [16]. The mass measurement of two channels and their combinations is summarised in the left of Figure 1. All measurements are in good agreement, and the combined Higgs mass is measured to be 125.11±0.09(stat.)±0.06(syst.) GeV.

## 3. Higgs width measurement

ATLAS and CMS measure the Higgs boson total width from off-shell and on-shell signal strength using $H \to ZZ^*$ decay mode in gluon-fusion (ggF) and VBF processes. The on-shell measurement depends on the Higgs total width from the Higgs propagator term. On the other hand, the off-shell measurement does not depend on the Higgs total width. In the off-shell phase space, the $gg \to H \to ZZ$ diagram destructively interferes with the $gg \to ZZ$ diagram in the leading-order in ggF. With the large interference effect, the off-shell signal strength can be measured. CMS (ATLAS) observe the significance of non-zero off-shell Higgs boson signal strength by 3.6(3.3) $\sigma$ and the CMS result is shown in the right of Figure 1. The off-sell signal strength is measured to be $0.62^{+0.68}_{-0.45}$ ($1.1^{+0.7}_{-0.6}$) for CMS (ATLAS). As stated above, the off-shell signal strength is expressed as

$\mu_{\text{off-shell}} \sim \kappa_g^2 \kappa_Z^2$ and the on-shell signal strength is expressed as $\mu_{\text{on-shell}} \sim \kappa_g^2 \kappa_Z^2 \frac{\Gamma_H^{\text{SM}}}{\Gamma_H}$, where $\kappa_g$ ($\kappa_Z$) represent the couplings between Higgs boson and gluon ($Z$ boson) normalised to the SM prediction. Assuming the couplings are the same in on-shell and off-shell processes, Higgs boson total width $\Gamma_H$ can be measured by $\frac{\mu_{\text{off-shell}}}{\mu_{\text{on-shell}}} \Gamma_H^{\text{SM}}$. The observed Higgs total width is $3.2^{+2.4}_{-1.7}$ ($4.5^{+3.3}_{-2.5}$) MeV for CMS (ATLAS), which is consistent with the SM Higgs total width, 4.1 MeV [17–20].

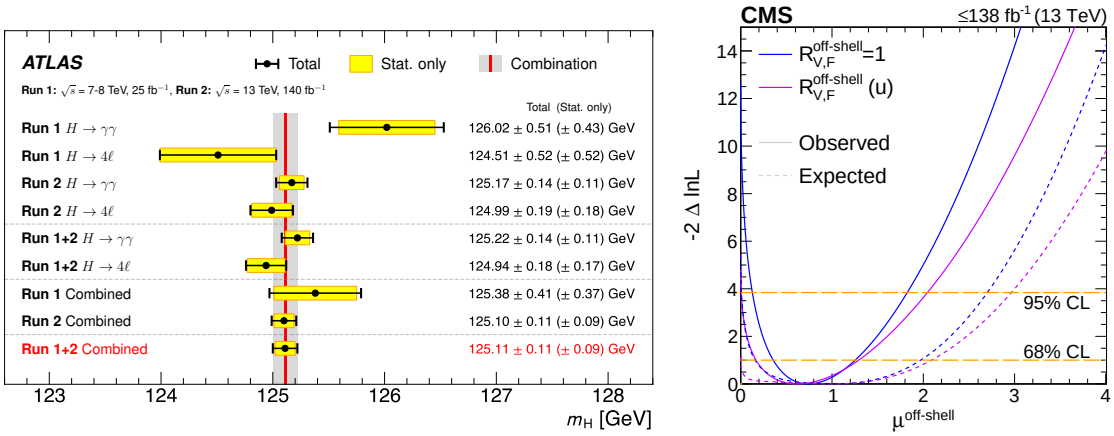


**Figure 1:** (Left) A summary of the Higgs boson mass measurement of the individual $H \to \gamma\gamma$ and $H \to ZZ \to 4\ell$ and the combination of two channels [14]. (Right) The likelihood profile as a function of the off-shell signal strength, $\mu_{\text{off-sell}}$ [19].

## 4. Higgs coupling and cross-section measurements

The measurements of couplings between the Higgs boson and the SM particles and non-SM particles are one of the most important Higgs properties measurements because many BSM models indicate the deviations from the SM. ATLAS and CMS measure the couplings in various production and decay modes which covers different couplings in the different phase spaces. The combined measurement of all productions and decay modes provides the most sensitive and comprehensive information on the couplings. Figure 2 shows the results of coupling measurement using $\kappa$-framework [21]. ATLAS and CMS have similar precision on the $\kappa$ parameters, which are coupling strength modifiers normalized by the coupling predicted by the SM. The precision for $\kappa_{W/Z}, \kappa_\gamma, \kappa_g, \kappa_\tau$ reaches 6-8% level, $\kappa_t, \kappa_b$ precision is approximately 10%, $\kappa_\mu$ precision is 20% and $\kappa_{Z\gamma}$ precision is 40% level [22, 23]. ATLAS also shows the limit on the branching fraction of invisible decay ($B_{\text{inv.}}$) and other undetected decay ($B_{\text{u.}}$) modes in Figure 2.

ATLAS measures the cross section using the simplified template cross section (STXS) framework [24]. The STXS defines the bins of kinematic regions for each production process. Figure 3 (left) shows the STXS measurements in 36 different phase space bins. The higher statistics of the dataset and the combination of various production and decay modes make the STXS measurement more sensitive to the BSM. Figure 3 (right) shows the constraint of Wilson coefficients of linearised SMEFT [25] using the combined STXS measurements [22]. The agreement with the SM expectation is 94.5% in the $p$-value.

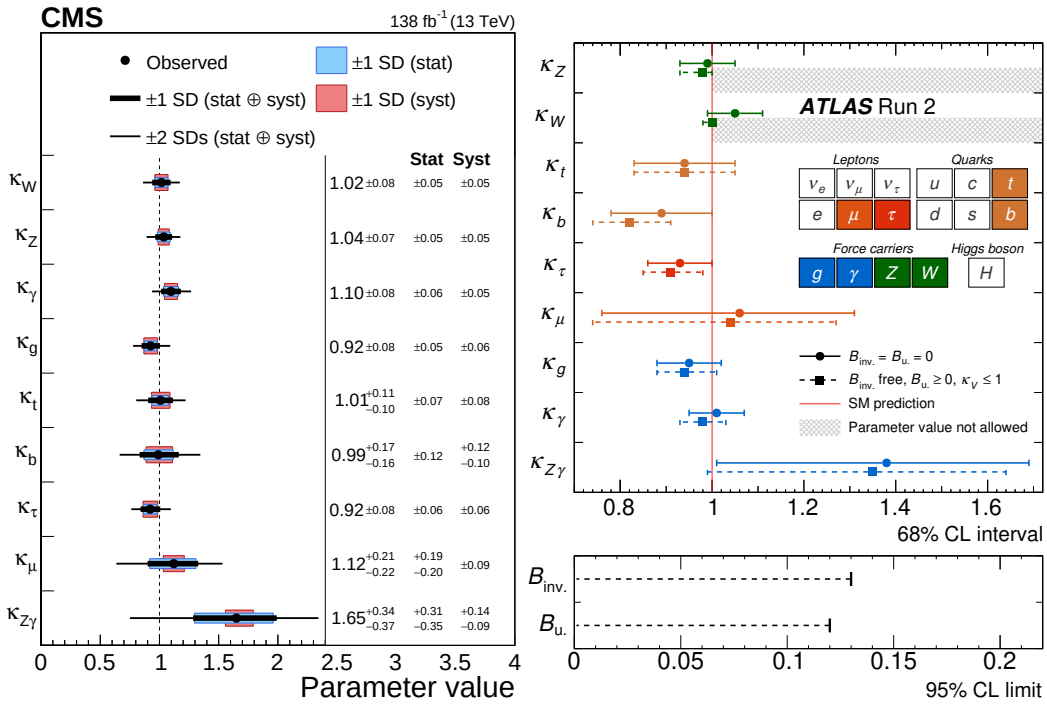


**Figure 2:** (Left) The combined coupling measurement and their uncertainties per particle and effective couplings of the photon, $Z\gamma$ and gluon assuming $B_{\text{inv.}} = B_{\text{u.}} = 0$ is shown [23]. (Right) In addition to that scenario, ATLAS also shows another scenario assuming $\kappa_V \leq 1$, $B_{\text{u.}} \geq 0$ and $B_{\text{inv.}}$ is free floated. The lower panel shows the 95% CL upper limits on $B_{\text{inv.}}$ and $B_{\text{u.}}$ [22].

CMS updates the property measurements of $ttH$ and $tH$ production processes using the full Run 2 dataset. A fully hadronic channel is newly analyzed in addition to the semi-leptonic and di-leptonic channels of $t\bar{t}$ decay and an artificial neural network is used to separate signal and background in all channels. The observed signal strength is $\mu_{ttH} = 0.33^{+0.26}_{-0.26}$, corresponding to the observed signal significance of $1.3\sigma$ with an expectation of 4.1 $\sigma$ [26]. Figure 4 (left) shows the simultaneous measurement of $\mu_{ttH}$ and $\mu_{tH}$. The best fit values of $\mu_{ttH}$ and $\mu_{tH}$ are 0.35 and $-3.83$, respectively [26].

ATLAS searches for new rare associated production of Higgs and $W$ bosons via vector boson fusion which is sensitive to the relative sign of the Higgs boson coupling of $W$ and $Z$ bosons. Figure 4 (middle) shows confidence intervals in the $\kappa_Z - \kappa_W$ plane. The negative scenario of the relative sign of the $\kappa_Z$ and $\kappa_W$ is excluded with significance of greater than $8\sigma$ [27].

ATLAS and CMS perform the combination of individual measurements of rare $Z\gamma$ decay modes. The observed individual signal strength is $\mu_{Z\gamma} = 2.0^{+1.0}_{-0.9}$ $(2.4^{+1.0}_{-0.9})$ for ATLAS (CMS) analyses [28, 29]. Figure 4 (right) shows the $Z\gamma$ mass distribution of events from all ATLAS and CMS analysis categories. The events are weighted by the $\ln(1 + S/B)$ of their categories, where $S$ and $B$ are the observed signal and background yields in the range $120 < m_{Z\gamma} < 130$ GeV. The signal strength in the combined measurement is $\mu_{Z\gamma} = 2.2 \pm 0.7$. The observed (expected) local significance with null hypothesis corresponds to 3.4 $\sigma$ (1.6 $\sigma$) [30]. The combined measurement provides the first evidence of the rare $Z\gamma$ decay modes. The $p$-value for the compatibility with the

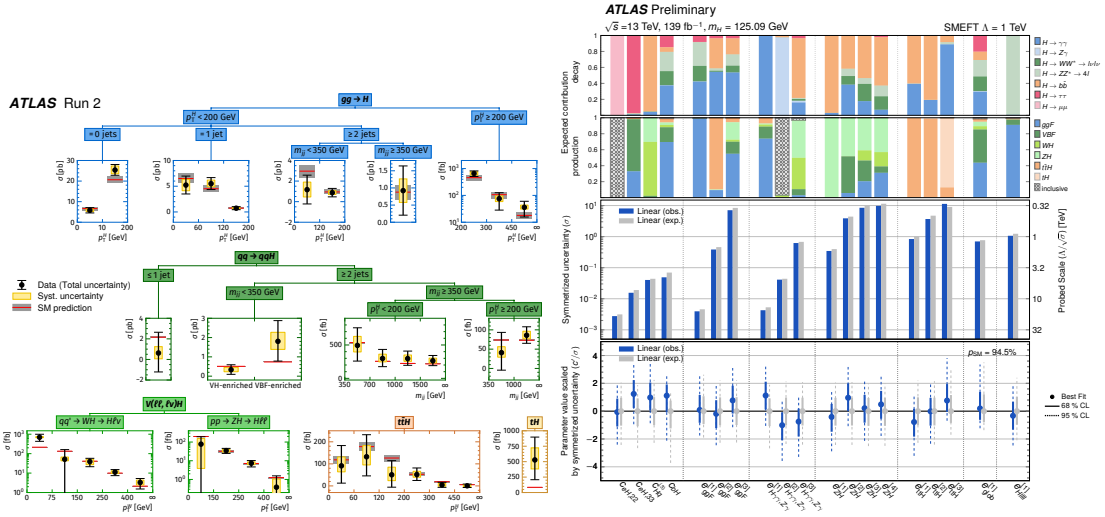


**Figure 3:** (Left) The observed and predicted Higgs boson production cross section in the different STXS bins [22]. (Right) The comparison of the observed and expected SMEFT parameters with a linearised model is shown in the bottom panel. The middle panel shows the 68% uncertainties on each parameter. The top panel shows the expected contribution of each production and decay mode [25].

SM is about 6%, and the observed local significance with respect to the SM is 1.9 $\sigma$ level.

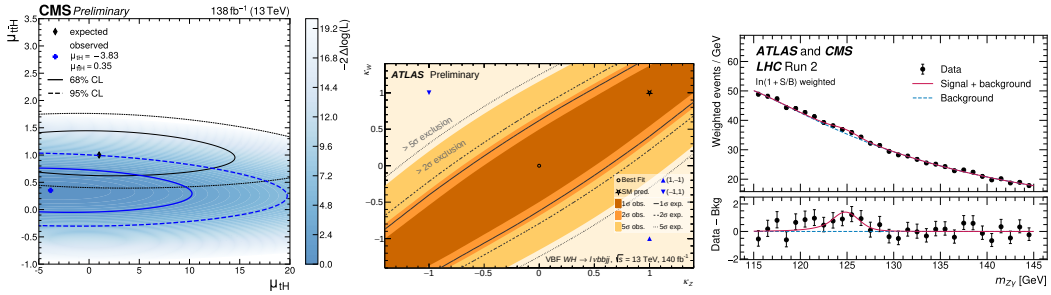


**Figure 4:** (Left) Simultaneous measurement of $\mu_{ttH}$ and $\mu_{tH}$ [26]. (Middle) Simultaneous fit results of $\kappa_W$ and $\kappa_Z$. The colored contours indicate the observed allowed regions in each significance [27]. (Right) The $Z\gamma$ mass distribution of events from all ATLAS and CMS analysis categories. The events are weighted by $\ln(1 + S/B)$ in each category [30].

## 5. New measurements using boosted topology

CMS has recently developed the reconstruction method using machine learning techniques for boosted Higgs boson which decays into a pair of bottom quarks. In the high-$p_{\mathrm{T}}^{H}$ topology, two $b$-quarks from the Higgs deacay are reconstructed as the one large-radius jet. DeepDoubleBvL-v2 (DDB) multivariate jet tagger [31] is applied to the gluon-fusion (ggF) and VBF events to improve the discrimination of Higgs candidates and QCD background and enhance the signal significance. Figure 5 shows the soft drop jet mass [33] distribution for ggF and VBF categories [32]. The

signal strength for the VBF process is measured to be $5.0^{+2.1}_{-1.8}$, which corresponds to the observed (expected) significance of 3.0 $\sigma$ (0.9 $\sigma$). For the ggF process, the signal strength is measured to be $2.1^{+1.9}_{-1.7}$, which corresponds to the observed (expected) significance of 1.2 $\sigma$ (0.9 $\sigma$).

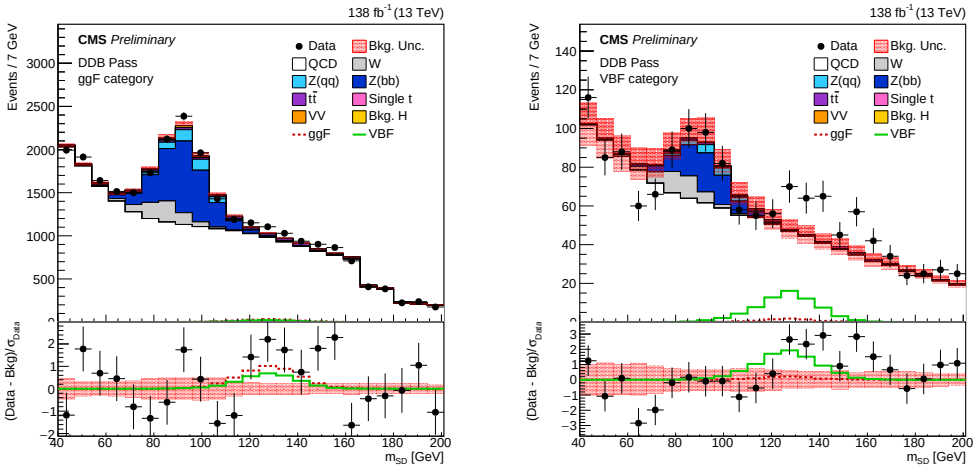


**Figure 5:** Soft-drop mass [33] distributions in ggF (left) and VBF (middle) categories [32].

## 6. Higgs pair production

The Higgs self-coupling measurement is one of the biggest goals of the LHC physics program since various BSM models indicate the deviation from the SM. The Higgs self-interaction is directly accessible via Higgs boson pair (HH) production. However, the HH production cross section is more than 1000 times lower than the single Higgs production cross section and very rare production at the LHC. Also, the Higgs boson self-interaction contributes to other processes via next-to-leading order EW corrections [34]. ATLAS and CMS search for the HH production process using various decay modes in ggF and VBF. Three main decay modes: $bb\gamma\gamma, bb\tau\tau, 4b$, are the most sensitive to the self-coupling measurement and their results are are combined in ATLAS. The observed (expected) upper limit on the double Higgs signal strength is set to 2.4 (2.9) at 95% CL. The observed values of $-2\ln(\Lambda)$ as a function of $\kappa_\lambda$ are shown in Figure 6 (left) for the single-Higgs and double-Higgs analyses, and their combination. The combined observed (expected) constraints on $\kappa_\lambda$ are $-0.4 < \kappa_\lambda < 6.3$ ($-1.9 < \kappa_\lambda < 7.6$) at 95% CL [34]. The observed and expected upper limit on VBF HH production cross section as a function of the quartic VVHH coupling modifier $\kappa_{2V}$ are shown in Figure 6 (right). The constraint on $\kappa_{2V}$ is in the range of 0.67 to 1.38. CMS excluded $k_{2V} = 0$ with a significance of 6.6 $\sigma$ [23].

## 7. First Run3 Higgs cross section measurements at 13.6 TeV

ATLAS measures inclusive and fiducial Higgs boson production cross-section in the $H \to \gamma\gamma$ and $H \to ZZ \to 4\ell$ [35] using approximately 30 fb$^{-1}$ of $pp$ collision data at a center-of-mass energy of $\sqrt{s} = 13.6$ TeV. The $m_{\gamma\gamma}$ and $m_{4\ell}$ distributions are shown in Figure 7 (right) and (middle).

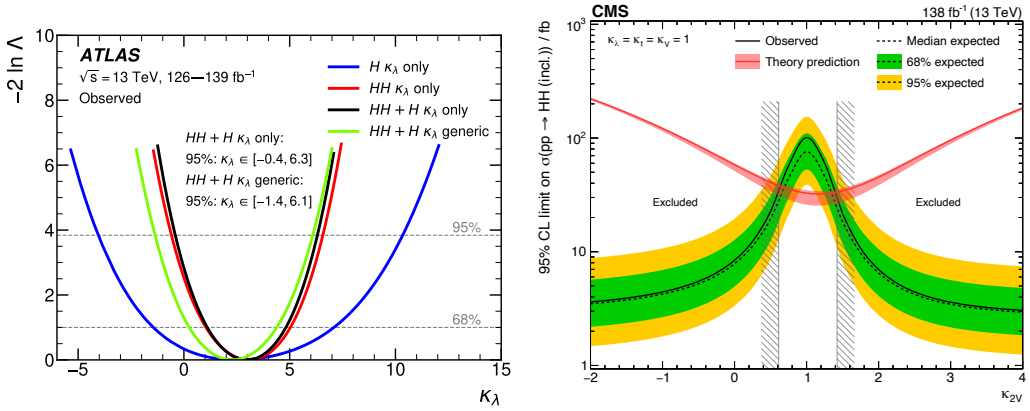


**Figure 6:** (Left) Observed values of the test statistic (-2ln(Λ)) as a function of $\kappa_\lambda$ parameter for the single-Higgs (blue) and double-Higgs (red) analysis, and their combinations in the scenarios assuming all other couplings fixed to unity (black), and assuming $\kappa_t, \kappa_b, \kappa_V$ and $\kappa_\tau$ are free floated [34]. (Right) Expected and observed 95% CL upper limit on the HH production cross section as a function of $\kappa_{2V}$ [23].

The total Higgs boson production cross-section at $\sqrt{s}$ = 13.6 TeV is measured to be $67^{+12}_{-11}$ pb for $H \to \gamma\gamma$ channel and 46 ± 12 pb for $H \to ZZ \to 4\ell$. The two measurements are compatible with a $p$-value of 20%. The total Higgs boson production cross-section combined with two channels is measured to be 58.2 ± 8.7 pb as shown in Figure 7 (right). All measurements are in good agreement with the SM prediction, 59.9 ± 2.6 pb.

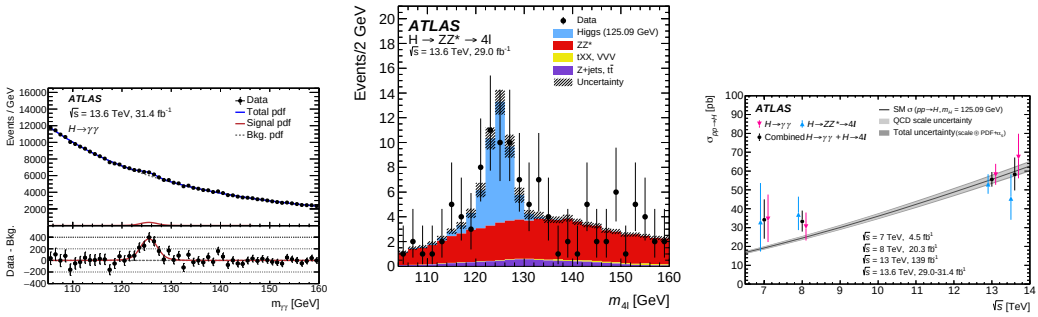


**Figure 7:** (Left) $m_{\gamma\gamma}$ distribution. (Middle) $m_{4\ell}$ distribution. (Right) The observed total cross section for each centre-of-mass energy from ATLAS Run 1, Run 2, and Run 3. The SM predictions and their uncertainties are shown as a function of centre-of-mass energy [35].

## 8. Conclusion

High statistics of the full Run 2 dataset collected by ATLAS and CMS at the LHC and improvement of the analysis techniques significantly improve the precision of Higgs boson property measurements. The precision of Higgs mass measurement reached less than 0.1%. The major couplings of Higgs boson are measured by less than 10% level. Higgs measurements for the rare

production processes and decay modes are accessible. ATLAS and CMS have evidence of rare decay mode, $H \to Z\gamma$ by 3.4 $\sigma$. The measurement of STXS and differential cross sections in the corner of phase spaces which is more sensitive to the BSM is doable due to large statistics and development of the boosted Higgs reconstruction techniques. The sensitivity of the Higgs pair production is improved dramatically during Run 2 and constrains to $\kappa_\lambda$ in the wide range. Furthermore, the first Run3 inclusive Higgs boson production cross section is measured by ATLAS and it is consistent with the SM prediction.

## References


[1] ATLAS Collaboration, *Observation of a new particle in the search for the standard model Higgs boson with the ATLAS detector at the LHC*, Phys. Lett. B 716 (2012) 1.

[2] CMS Collaboration, *Observation of a new boson at a mass of 125 GeV with the CMS experiment at the LHC*, Phys. Lett. B 716 (2012) 30.

[3] L. Evans and P. Bryant (editors), *LHC Machine*, 2008 JINST 3 S08001.

[4] ATLAS Collaboration, *The ATLAS Experiment at the CERN Large Hadron Collider*, JINST 3 (2008) S08003.

[5] CMS Collaboration, *The CMS experiment at the CERN LHC*, JINST 3 (2008) S08004.

[6] ATLAS Collaboration, *Observation of Higgs boson production in association with a top quark pair at the LHC with the ATLAS detector*, Phys.Lett.B 784 (2018) 173-191.

[7] CMS Collaboration, *Observation of $t\bar{t}H$ production*, Phys.Rev.Lett. 120 (2018) 23, 231801.

[8] ATLAS Collaboration, *Observation of $H \to b\bar{b}$ decays and $VH$ production with the ATLAS detector*, Phys.Lett.B 786 (2018) 59-86.

[9] CMS Collaboration, *Observation of Higgs boson decay to bottom quarks*, Phys.Rev.Lett. 121 (2018) 12, 121801.

[10] ATLAS Collaboration, *A search for the dimuon decay of the Standard Model Higgs boson with the ATLAS detector*, Phys.Lett.B 812 (2021) 135980.

[11] CMS Collaboration, *Evidence for Higgs boson decay to a pair of muons*, JHEP 01 (2021) 148.

[12] ATLAS Collaboration, *Evidence for Higgs boson decays to a low-mass dilepton system and a photon in pp collisions at $\sqrt{s}$=13 TeV with the ATLAS detector*, Phys.Lett.B 819 (2021) 136412.

[13] ATLAS Collaboration, *The ATLAS Experiment at the CERN Large Hadron Collider: A Description of the Detector Configuration for Run 3*, arXiv:2305.16623 [hep-ex].

[14] ATLAS Collaboration, *Measurement of the Higgs boson mass with $H \to \gamma\gamma$ decays in 140 $fb^{-1}$ of $\sqrt{s}$ = 13 TeV $pp$ collisions with the ATLAS detector*, arXiv:2308.07216 [hep-ex].

[15] ATLAS Collaboration, *Electron and photon energy calibration with the ATLAS detector using LHC Run 2 data*, arXiv:2309.05471 [hep-ex].

[16] ATLAS Collaboration, *Combined measurement of the Higgs boson mass from the $H \to \gamma\gamma$ and $H \to ZZ^* \to 4\ell$ decay channels with the ATLAS detector using $\sqrt{s}$ = 7, 8 and 13 TeV $pp$ collision data*, arXiv:2308.04775 [hep-ex].

[17] ATLAS Collaboration, *Evidence of off-shell Higgs boson production from ZZ leptonic decay channels and constraints on its total width with the ATLAS detector*, Phys.Lett.B 846 (2023) 138223.

[18] ATLAS Collaboration, *Higgs boson production cross-section measurements and their EFT interpretation in the $4\ell$ decay channel at $\sqrt{s}$ =13 TeV with the ATLAS detector*, Eur.Phys.J.C 81 (2021) 5, 398.

[19] CMS Collaboration, *Measurement of the Higgs boson width and evidence of its off-shell contributions to ZZ production*, Nature Phys. 18 (2022) 11, 1329-1334.

[20] CMS Collaboration, *Constraints on anomalous Higgs boson couplings to vector bosons and fermions in its production and decay using the four-lepton final state*, Phys.Rev.D 104 (2021) 5, 052004.

[21] LHC Higgs Cross Section Working Group, *Handbook of LHC Higgs Cross Sections: 3. Higgs Properties*, Report No. CERN-2013-004 (CERN, 2013); https://doi.org/10.5170/CERN-2013-004.

[22] ATLAS Collaboration, *A detailed map of Higgs boson interactions by the ATLAS experiment ten years after the discovery*, Nature 612 (2022) 7941, E24.

[23] CMS Collaboration, *A portrait of the Higgs boson by the CMS experiment ten years after the discovery*, Nature 607 (2022) 7917, 60-68.

[24] LHC Higgs Cross Section Working Group, *Handbook of LHC Higgs Cross Sections: 4. Deciphering the Nature of the Higgs Sector*, Report No. CERN-2017-002 (CERN, 2017); https://doi.org/10.23731/CYRM-2017-002.

[25] ATLAS Collaboration, *Interpretations of the ATLAS measurements of Higgs boson production and decay rates and differential cross-sections in $pp$ collisions at $\sqrt{s}$ = 13 TeV*, ATLAS-CONF-2023-052, https://cds.cern.ch/record/2870216

[26] CMS Collaboration, *Measurement of the $t\bar{t}H$ and $tH$ production rates in the $H \to b\bar{b}$ decay channel with* 138 $\text{fb}^{-1}$ *of proton-proton collision data at* $\sqrt{s}$ = 13 TeV, CMS-PAS-HIG-19-011, https://cds.cern.ch/record/2868175

[27] ATLAS Collaboration, *Determining the relative sign of the Higgs boson couplings to W and Z bosons using VBF WH production with the ATLAS detector*, ATLAS-CONF-2023-057, http://cds.cern.ch/record/2870224.

[28] ATLAS Collaboration, *A search for the $Z\gamma$ decay mode of the Higgs boson in $pp$ collisions at $\sqrt{s}$ = 13 TeV with the ATLAS detector*, Phys.Lett.B 809 (2020) 135754.

[29] CMS Collaboration, *Search for Higgs boson decays to a Z boson and a photon in proton-proton collisions at $\sqrt{s}$ = 13 TeV*, JHEP 05 (2023) 233.

[30] CMS and ATLAS Collaborations, *Evidence for the Higgs boson decay to a Z boson and a photon at the LHC*, arXiv:2309.03501 [hep-ex].

[31] CMS Collaboration, *Performance of the mass-decorrelated DeepDoubleX classifier for double-b and double-c large-radius jets with the CMS detector*, CMS-DP-2022-041, https://cds.cern.ch/record/2839736

[32] *Search for boosted Higgs bosons produced via vector boson fusion in the $H \to b\bar{b}$ decay mode using LHC proton-proton collision data at $\sqrt{s}$ = 13 TeV*, CMS-PAS-HIG-21-020, https://cds.cern.ch/record/2866501

[33] A. J. Larkoski, S. Marzani, G. Soyez, and J. Thaler, *Soft drop*, JHEP 05 (2014) 146.

[34] ATLAS Collaboration, *Constraints on the Higgs boson self-coupling from single- and double-Higgs production with the ATLAS detector using pp collisions at s=13 TeV*, Phys.Lett.B 843 (2023) 137745.

[35] ATLAS Collaboration, *Measurement of the $H \to \gamma\gamma$ and $H \to ZZ^* \to 4\ell$ cross-sections in $pp$ collisions at $\sqrt{s}$ = 13.6 TeV with the ATLAS detector*, arXiv:2306.11379 [hep-ex].